Specific heat, internal energy, and thermodynamic Casimir force in the neighborhood of the λ transition

Martin Hasenbusch*
Institut für Physik, Humboldt-Universität zu Berlin, Newtonstr. 15, 12489 Berlin, Germany
(Received 26 January 2010; revised manuscript received 12 March 2010; published 7 April 2010)

We discuss the relation of the excess specific heat, the excess energy per area, and the thermodynamic Casimir force in thin films. *A priori* these quantities depend on the reduced temperature t and the thickness L_0 of the film. However finite-size scaling theory predicts that the scaling functions $h''(x)$, $h'(x)$, and $\theta(x)$ of these quantities depend only on the combination $x=t[L_0/\xi_0]^{1/\nu}$, where ν is the critical exponent and ξ_0 the amplitude of the correlation length. Furthermore, the finite-size scaling function $\theta(x)$ of the thermodynamic Casimir force per area can be expressed in terms of the scaling functions $h'(x)$ and $h(x)$ of the excess energy per area and the excess free energy per area. Here we study this relation at the example of thin films of the improved two-component ϕ^4 model on the simple cubic lattice. Note that this model undergoes a second-order phase transition that belongs to the three-dimensional XY universality class. First we simulate films with periodic boundary conditions in the short direction and a thickness up to $L_0=13$ lattice spacings. We find that even for these rather thin films, the predictions of finite-size scaling are well satisfied. We repeat the analysis for films with free boundary conditions. To this end we use Monte Carlo data for the energy per area obtained in previous work. It turns our that corrections to scaling caused by the boundary conditions are very prominent in this case. Only by taking into account these corrections we are able to obtain $\theta(x)$ from the excess energy. Finally we repeat this exercise using experimental data for the excess specific heat of ^{4}He films near the λ transition. The finite-size scaling behavior of the excess specific heat is governed by $h''(x)$, which is proportional to the scaling function f_2 discussed in the literature.

DOI: 10.1103/PhysRevB.81.165412 PACS number(s): 05.50.+q, 05.70.Jk, 05.10.Ln

I. INTRODUCTION

In 1978 Fisher and de Gennes[1] realized that when thermal fluctuations are restricted by a container a force acts on the walls of the container. Since this effect is rather similar to the Casimir effect, where the restriction of quantum fluctuations induces a force, it is called "thermodynamic" Casimir effect. Since thermal fluctuations only extend to large scales in the neighborhood of a continuous phase transitions it is also called "critical" Casimir effect. Recently this effect has attracted much attention since it could be verified for various experimental systems and quantitative predictions could be obtained from Monte Carlo simulations of spin models.[2]

In the thermodynamic limit of the three-dimensional system, the correlation length, which measures the spatial extension of fluctuations, diverges following the power law

$$\xi \simeq \xi_{0,\pm}|t|^{-\nu}, \tag{1}$$

where $t=(T-T_c)/T_c$ is the reduced temperature and T_c the critical temperature. $\xi_{0,+}$ and $\xi_{0,-}$ are the amplitudes of the correlation length in the high- and low-temperature phase, respectively. The symbol $\simeq$ means asymptotically equal; corrections vanish as $t\to 0$. While $\xi_{0,+}$ and $\xi_{0,-}$ depend on the microscopic details of the system, the critical exponent ν and the ratio $\xi_{0,+}/\xi_{0,-}$ are universal. At the critical point also other quantities such as the specific heat show a singular behavior,

$$C \simeq A_{\pm}|t|^{-\alpha} + B. \tag{2}$$

In the case of the XY universality class that we consider here, the exponent $\alpha=-0.151(3)$ (Ref. 3) of the specific heat is negative. Therefore the analytic background B has to be taken into account. Note that the critical exponents of the correlation length and the specific heat are related by the hyperscaling relation $\alpha=2-d\nu$, where d is the dimension of the system. For reviews on critical phenomena and its modern theory, the renormalization group (RG), see, e.g., Refs. 4–7.

The singular behavior at the critical point originates from the fact that thermal fluctuations range over all length scales. Therefore the behavior in the neighborhood of the critical point is modified if the system is confined by a container. *A priori* thermodynamic quantities are functions of the reduced temperature and the size L_0 of the container, assuming a fixed geometry. However the theory of finite-size scaling[8,9] predicts that the physics of the system is governed by the ratio L_0/ξ as long as $L_0, \xi \gg a$, where a is the microscopic scale of the system. In particular, if a quantity in the thermodynamic limit behaves as $A \simeq a_{0,\pm}|t|^{-w}$, finite-size scaling predicts that $A(L_0,t) \simeq L_0^{w/\nu}\tilde{g}(L_0/\xi)$, where w is the critical exponent of A and ξ the correlation length of the bulk system. We can rewrite this equation as

$$A(L_0,t) \simeq L_0^{w/\nu} g(t[L_0/\xi_{0,+}]^{1/\nu}) \tag{3}$$

by using Eq. (1), which is the form used in the following. Note that in Eq. (3) we take $\xi_{0,+}$ for both $t \geq 0$ and $t<0$. Choosing $\xi_{0,+}$ and not $\xi_{0,-}$ here, we follow the literature. Typically $\xi_{0,+}$ can be more accurately determined than $\xi_{0,-}$. Below ξ_0 always means $\xi_{0,+}$. Note that the function g depends on the geometry of the container and on the type of boundary conditions that is imposed by its walls on the order parameter of the system.

The predictions of finite-size scaling theory have been tested in experiments and theoretical studies for various universality classes and confining geometries; for reviews see Refs. 8 and 9. Here we shall focus on thin films in the three-dimensional XY universality class, which is shared by the λ transition of ^{4}He. Very precise experimental results for critical exponents and universal amplitude ratios were obtained for this phase transition.[10] Also a large number of experiments on thin films of ^{4}He and ^{3}He-^{4}He mixtures were performed to probe finite-size scaling.[11] In particular, the specific heat of thin films has been studied. The excess specific heat should behave as

$$C_{bulk}(t) - C(L_0,t) \simeq L_0^{\alpha/\nu} f_2(t[L_0/\xi_0]^{1/\nu}). \tag{4}$$

The reason to study the excess specific heat rather than just the specific heat $C(L_0,t)$ is to cancel the analytic background B. Note that the scaling function $f_2(x)$ of the excess specific heat is, up to a constant factor, the second derivative $h''(x)$ of the scaling function $h(x)$ of the excess free energy per area

$$\tilde{f}_{ex} = \tilde{f}_{film}(L_0,t) - L_0 \tilde{f}_{bulk}(t) \simeq k_B T L_0^{-d+1} h(t[L_0/\xi_0]^{1/\nu}), \tag{5}$$

where $\tilde{f}_{film}(L_0,t)$ is the free energy per area of the thin film, $\tilde{f}_{bulk}(t)$ the free energy density of the bulk system, $d=3$ the dimension of the system. Note that in the case of thin films we consider, following the literature on the thermodynamic Casimir effect, free energies per area. We hope that this does not lead to confusion, since in the case of the specific heat, energies per volume are considered.

From a thermodynamic point of view, the thermodynamic Casimir force per area is given by

$$F_{Casimir} = -\frac{\partial \tilde{f}_{ex}}{\partial L_0}, \tag{6}$$

where L_0 is the thickness of the film. Inserting the finite-size scaling ansatz (5) for the excess free energy into Eq. (6) we get

$$\begin{aligned} F_{Casimir} &\simeq -k_B T \frac{\partial (L_0^{-2} h[t(L_0/\xi_0)^{1/\nu}])}{\partial L_0} \\ &= -k_B T L_0^{-3} \left\{ -2h[t(L_0/\xi_0)^{1/\nu}] \right. \\ &\quad \left. + \frac{1}{\nu} t[L_0/\xi_0]^{1/\nu} h'[t(L_0/\xi_0)^{1/\nu}] \right\} \\ &= k_B T L_0^{-3} \theta[t(L_0/\xi_0)^{1/\nu}], \end{aligned} \tag{7}$$

where

$$\theta(x) = 2h(x) - \frac{x}{\nu} h'(x). \tag{8}$$

This relation is well known and can be found, e.g., in Ref. 12. We like to emphasize that Eq. (7) relies on the fundamental assumption that finite-size scaling functions depend only on the scaling variable $x=t[L_0/\xi_0]^{1/\nu}$ and not on t and L_0 separately. The amazing consequence is that apparently completely different physical quantities such as the thermodynamic Casimir force and the excess specific heat of thin films are governed by the same scaling function $h(x)$.

The purpose of the present work is to probe Eqs. (7) and (8) using numerical data from Monte Carlo simulations of a lattice model and experimental data obtained for films of ^{4}He. To this end we compute $h'(x)$ from data for the excess energy or $h''(x)$ from data for the excess specific heat. Using numerical integration we then arrive at estimates for $h(x)$ or $h'(x)$ and $h(x)$, respectively. Using Eqs. (7) and (8) we finally arrive at an estimate for $\theta(x)$. This estimate is compared with $\theta(x)$ computed from data for the thermodynamic Casimir force, Eq. (6). The mismatch of these two estimates of $\theta(x)$ allows us to quantify corrections to scaling that have not been taken into account in the analysis of the data. Or, if these deviations do not decrease with increasing thickness L_0 of the film, disprove finite-size scaling.

First we have studied films with periodic boundary conditions. To this end we have simulated the improved two-component ϕ^4 model on the simple cubic lattice, where improved means that leading corrections $\propto L_0^{-\omega}$, with $\omega \approx 0.8$, are eliminated. We find that corrections to scaling are small for the lattices sizes $L=8$, 9, 12, and 13 that we have simulated. Also the results for $\theta(x)$ obtained by the two alternative approaches are consistent. We compare our final result for the scaling function $\theta(x)$ for periodic boundary conditions with previous Monte Carlo simulations[13,14] and field theoretic results.[15,16]

Next we analyze data for the energy density that were obtained in Ref. 17 from simulations of the improved two-component ϕ^4 model on the simple cubic lattice. In Ref. 17 these data were used to compute the specific heat. In order to get a vanishing order parameter as it is observed at the boundaries of ^{4}He films, Dirichlet boundary conditions with vanishing field were imposed. In singular quantities these lead to corrections $\propto L_0^{-1}$,[18] which can be expressed by an effective thickness $L_{0,eff}=L_0+L_s$. In Ref. 19 we find $L_s = 1.02(7)$ for the model that we consider here. Note that the boundary conditions also affect the analytic background of the specific heat and the energy density, which also leads to corrections $\propto L_0^{-1}$. However it turns out that these corrections are not given by the same $L_{0,eff}$ as for the singular quantities. Taking into account these subtleties we arrive at accurate results for $h'(x)$, $h(x)$, and $\theta(x)$. In particular, for $\theta(x)$ in the range $-15 \lessapprox x \lessapprox 4$ we find a good match with our previous result,[20,21] where we computed the Casimir force by taking the derivative of the excess free energy with respect to the thickness L_0 of the film. In Ref. 20 we have compared our result for $\theta(x)$ with previous ones obtained from simulations of the XY model[14,22,23] and experiments on thin films of ^{4}He;[24,25] overall we find a reasonable agreement.

Finally we compute $\theta(x)$ by using experimental results for the excess specific heat obtained from experiments on thin films of ^{4}He.[26,27] For $-5 \lessapprox x \lessapprox 4$ we find a reasonable match with our result,[20] which is essentially consistent with the experiments on the thermodynamic Casimir force.[24,25] However in the low-temperature phase, for $x \lessapprox -5$ we get results that strongly deviate from Ref. 20 and can even be ruled out by plausibility. This corroborates the observation that in the low-temperature phase for $x \lessapprox -5$ the data for the excess specific heat do not scale well.[11]

This paper is organized as follows: first we define the model and the observables that we consider. Next we discuss

the finite-size scaling behavior of the free energy per area. In particular, we discuss corrections to scaling caused by Dirichlet boundary conditions. In Sec. IV we analyze our Monte Carlo data for films with periodic boundary conditions. In Sec. V we compute $h'(x)$, $h(x)$, and $\theta(x)$ using the data for the energy per area of thin films with Dirichlet boundary conditions obtained in Ref. 17. The result for $\theta(x)$ is compared with the one that we[20] obtained directly from the thermodynamic Casimir force. Next in Sec. VI we compute $\theta(x)$ starting from data for the excess specific heat of films of ^{4}He in the neighborhood of the λ transition. Finally we summarize and conclude.

II. MODEL AND THE OBSERVABLES

We study the two-component ϕ^4 model on the simple cubic lattice. We label the sites of the lattice by $x=(x_0,x_1,x_2)$. The components of x might assume the values $x_i \in \{1,2,\ldots,L_i\}$. We study the thin-film geometry characterized by $L_0 \ll L_1=L_2=L$. In this work we have simulated lattices with periodic boundary conditions in all three directions. Furthermore we analyze data obtained in Ref. 17 for thin films with free boundary conditions in the zero direction. The Hamiltonian of the two-component ϕ^4 model, for a vanishing external field, is given by

$$\mathcal{H} = -\beta \sum_{\langle x,y \rangle} \vec{\phi}_x \cdot \vec{\phi}_y + \sum_x [\vec{\phi}_x^2 + \lambda(\vec{\phi}_x^2 - 1)^2], \tag{9}$$

where the field variable $\vec{\phi}_x$ is a vector with two real components. $\langle x,y \rangle$ denotes a pair of nearest-neighbor sites on the lattice. The partition function is given by

$$Z = \prod_x \left[\int d\phi_x^{(1)} \int d\phi_x^{(2)} \right] \exp(-\mathcal{H}). \tag{10}$$

Note that following the conventions of our previous work, e.g., Ref. 28 we have absorbed the inverse temperature β into the Hamiltonian. Therefore, following Ref. 6 we actually should call it reduced Hamiltonian. In the limit $\lambda \to \infty$ the field variables are fixed to unit length; hence the XY model is recovered. For $\lambda=0$ we get the exactly solvable Gaussian model. For $0<\lambda\leq\infty$ the model undergoes a second-order phase transition that belongs to the XY universality class. Numerically, using Monte Carlo simulations and high-temperature series expansions, it has been shown that there is a value $\lambda^*>0$, where leading corrections to scaling vanish. Numerical estimates of λ^* given in the literature are $\lambda^*=2.10(6)$,[29] $\lambda^*=2.07(5)$,[28] and most recently $\lambda^*=2.15(5)$.[3] The inverse of the critical temperature β_c has been determined accurately for several values of λ using finite-size scaling.[3] We shall perform our simulations at $\lambda=2.1$ since for this value of λ comprehensive Monte Carlo studies of the three-dimensional system in the low- and the high-temperature phase have been performed.[3,19,30,31] At $\lambda=2.1$ one gets $\beta_c=0.5091503(6)$.[3] Since $\lambda=2.1$ is not exactly equal to λ^*, there are still corrections $\propto L^{-\omega}$, although with a small amplitude. In fact, following,[3] it should be by at least a factor 20 smaller than for the standard XY model.

In Ref. 19 we find for $\lambda=2.1$ by fitting the data for the second moment correlation length in the high-temperature phase $\xi_{2nd} \simeq 0.26362(8) t^{-0.6717}$, where $t=0.5091503-\beta$. We shall use this definition of the reduced temperature also in the following discussion of our numerical results; Hence $\xi_0=0.26362(8)$. Note that in the high-temperature phase there is little difference between ξ_{2nd} and the exponential correlation length ξ_{exp} which is defined by the asymptotic decay of the two-point correlation function. Following[28] $\lim_{t\to 0} \frac{\xi_{exp}}{\xi_{2nd}} = 1.000204(3)$ for the thermodynamic limit of the three-dimensional system. Hence at the level of precision reached here it does not matter whether $\xi_{0,exp}$ or $\xi_{0,2nd}$ is used in the scaling variable $x=t[L_0/\xi_0]^{1/\nu}$.

Internal energy and the free energy

The reduced free energy density is defined as

$$f = -\frac{1}{L_0 L_1 L_2} \ln Z. \tag{11}$$

This means that compared with the free energy density $\tilde{f}$, a factor $k_B T$ is skipped.

Note that in Eq. (9) β does not multiply the second term. Therefore, strictly speaking, β is not the inverse of $k_B T$. In order to study universal quantities it is not crucial how the transition line in the β-λ plane is crossed, as long as this path is not tangent to the transition line. Therefore, following computational convenience, we vary β at fixed λ. Correspondingly we define the (internal) energy density as the derivative of the reduced free energy density with respect to β. Furthermore, to be consistent with our previous work,[17] we multiply by −1,

$$E = \frac{1}{L_0 L_1 L_2} \frac{\partial \ln Z}{\partial \beta}. \tag{12}$$

It follows

$$E = \frac{1}{L_0 L_1 L_2} \left\langle \sum_{\langle x,y \rangle} \vec{\phi}_x \cdot \vec{\phi}_y \right\rangle, \tag{13}$$

which can be easily determined in Monte Carlo simulations. From Eqs. (11) and (12) it follows that the free energy density can be computed as

$$f(\beta) = f(\beta_0) - \int_{\beta_0}^{\beta} d\tilde{\beta} E(\tilde{\beta}). \tag{14}$$

In the context of thin films we consider energies and free energies per area. Also these are denoted by E and f. This should not lead to confusion since it is always clearly indicated in the text.

III. FINITE-SIZE SCALING BEHAVIOR OF THE FREE ENERGY

Let us briefly discuss the scaling behavior of the reduced excess free energy per area. Since we study an improved model we ignore corrections $\propto L_0^{-\omega}$ in the following. We take into account leading corrections due to free boundary conditions by replacing the thickness L_0 of the film by $L_{0,eff}=L_0$

$+L_s$ at the appropriate places. We split the free energies in singular (s) and nonsingular (ns) parts,

$$f_{ex}(t,L_0) = f_{film}(t,L_0) - L_0 f_{bulk}(t) = f_{film,s}(t,L_0) + L_{0,eff,ns} f_{ns}(t) - L_0 f_{bulk,s}(t) - L_0 f_{ns}(t) = L_{0,eff}^{-2} h(x) + L_s f_{bulk,s}(t) + L_{sns} f_{ns}(t), \quad (15)$$

where

$$h(x) = L_{0,eff}^2 [f_{film,s}(t,L_0) - L_{0,eff} f_{bulk,s}(t)] \quad (16)$$

is a universal finite-size scaling function and $x = t[L_{0,eff}/\xi_0]^{1/\nu}$. Following RG theory the nonsingular part is not affected by finite-size effects. However it is not clear *a priori* how Dirichlet boundary conditions affect the nonsingular part of the free energy. Therefore we allow for $L_{sns} = L_{0,eff,ns} - L_0 \neq 0$ and $L_{sns} \neq L_s$. Taking the derivative with respect to L_0 we get the thermodynamic Casimir force per area[12]

$$\beta F_{Casimir} = -\frac{\partial f_{ex}(t,L_0)}{\partial L_0} = 2L_{0,eff}^{-3} h(x) - L_{0,eff}^{-3} \frac{1}{\nu} x h'(x) = L_{0,eff}^{-3} \theta(x), \quad (17)$$

where

$$\theta(x) = 2h(x) - \frac{1}{\nu} x h'(x). \quad (18)$$

Note that the boundary terms $L_s f_{bulk,s}$ and $L_{sns} f_{ns}$ do not contribute to the Casimir force.

IV. FILMS WITH PERIODIC BOUNDARY CONDITIONS

As preparation we have studied films with periodic boundary conditions in all directions. In contrast to free boundary conditions, there are no corrections to finite-size scaling caused by the boundaries. Therefore the analysis of the data should be much simpler for periodic boundary conditions than for free ones.

We have simulated films of the thicknesses $L_0=8$, 9, 12, and 13. First we have located the Kosterlitz-Thouless (KT) transition[32] of the films. To this end we have used the matching method discussed in Ref. 33 and applied to thin films with free boundary conditions in Ref. 19.

Then we have simulated the films for a large number of β values in the critical region. We have measured the energy per area of the films. Using the energy density of the three-dimensional bulk system obtained in Ref. 17 we obtain the excess energy per area. Using these data, we compute the finite scaling functions $h'(x)$ and $h(x)$. By using Eq. (8) we obtain $\theta(x)$. For comparison we have computed the thermodynamic Casimir force by using Eq. (6). To this end, we have approximated the derivative of the excess free energy per area by finite differences.

In our simulations one update cycle consists of one Metropolis sweep, two over-relaxation sweeps and a number of single cluster[34] updates. As random number generator we have used the SIMD-oriented Fast Mersenne Twister algorithm.[35]

A. Kosterlitz-Thouless transition

The basic idea of the matching method discussed in Ref. 33 is to compare the finite-size scaling behavior of the Binder cumulant U_4 and the second moment correlation length over the lattice size ξ_{2nd}/L in thin films with that of two-dimensional XY models at the KT transition. To this end we have simulated lattices of the sizes 8×800^2, 9×800^2, 12×1200^2, and 13×1200^2. As check, we have simulated in addition a lattice of the size 12×480^2. We performed about 10^5 update cycles in each case. These simulations took about 2 month of CPU time on a single core of a Quad-Core Opteron™ 2378 CPU (2.4 GHz). We find $\beta_{KT}=0.52705(2)$, 0.52413(2), 0.51888(2), and 0.51778(2), for $L_0=8$, 9, 12, and 13, respectively. Note that our estimates of β_{KT} for $L_0=12$ obtained from $L=480$ and $L=1200$ are consistent within error bars. These results correspond to $x_{KT}=[\beta_c - \beta_{KT}][L_0/\xi_0]^{1/\nu}=-2.880(3)$, $-2.872(4)$, $-2.863(6)$, and $-2.860(7)$. These results vary only little with L_0, indicating that corrections to scaling are numerically small. We quote $x_{KT}=-2.86(2)$ as result for the scaling limit $L_0\to\infty$.

This result can be compared with that of Schultka and Manousakis[36] who have studied the standard XY model. They have simulated films with periodic boundary conditions of the thicknesses $L_0=3$, 4, 6, 8, 10, and 12. They find for the scaling limit $L_0^{1/\nu}[T_{KT}-T_c]/T_c=-0.9965(9)$. Using $\xi_0=0.4894(5)$ (Ref. 19) we arrive at $x_{KT}=-2.887(1)$, which is in reasonable agreement with our present result. Note that in the case of free boundary conditions, in the scaling limit, the KT transition takes place at $x_{KT}=-7.48(3)$.[19]

B. Scaling functions of the excess energy and the thermodynamic Casimir force

In our simulations we determined the energy $E(L_0,\beta)$ per area for lattices of the thicknesses $L_0=8$, 9, 12, and 13 for a large number of β values in the neighborhood of the critical temperature. In particular, we have simulated $L_0=8$ and 9 at 55 β values in the interval $0.35\le\beta\le0.565$ and $L_0=12$ and 13 at 73 β values in the interval $0.42\le\beta\le0.568$. We have used large values of L to keep finite L effects under control. In particular, for $L_0=12$ and 13 we have simulated lattices up to $L=2400$. We performed 10^5 up to 10^6 update cycles, depending on the lattice size. In total we have used about 4 month of CPU time on a single core of a Quad-Core Opteron™ 2378 CPU (2.4 GHz). In order to compute the excess energy per area

$$E_{ex}(L_0,\beta) = E(L_0,\beta) - L_0 E_{bulk}(\beta) \quad (19)$$

we have used the results for $E_{bulk}(\beta)$ obtained in Sec. 4.1 of Ref. 17. In Fig. 1 our results for $E_{ex}L_0^2[L_0/\xi_0]^{-1/\nu}$ are plotted as a function of $t[L_0/\xi_0]^{1/\nu}$. The data points for $L_0=8$, 9, 12, and 13 fall nicely on top of each other.

Next we have computed the scaling function $\theta(x)$ by using Eq. (8). To this end we have integrated $h'(x) \simeq E_{ex}L_0^2[L_0/\xi_0]^{-1/\nu}$ by using the trapezoidal rule to obtain the scaling function of the excess free energy per area $h(x)$. We have started the integration at $x\approx25$ in the high-temperature phase, where $h'(x)$ is vanishing within our statistical errors. In order to estimate the systematical error due to the finite

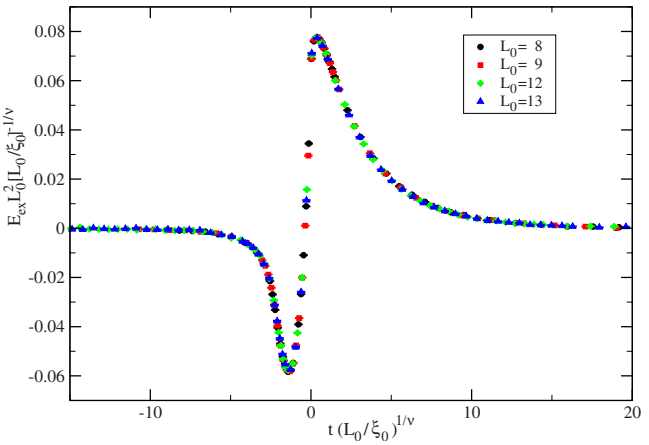

FIG. 1. (Color online) We plot $E_{ex}L_0^2[L_0/\xi_0]^{-1/\nu}$ as a function of $t[L_0/\xi_0]^{1/\nu}$ for L_0=8, 9, 12, and 13 for periodic boundary conditions. For a discussion see the text.

step size of the trapezoidal rule we have redone the integration, skipping every second value of x; i.e., doubling the step size. We find that the results are consistent within the statistical errors. Therefore the systematical error due to the finite step size should be of similar size or smaller than the statistical one.

The results for $\theta(x)$ are given in Fig. 2. The data points for L_0=8, 9, 12, and 13 fall nicely on top of each other. This is not too surprising since already for the excess energy we have seen a very good collapse of the data.

Next we have computed

$$\Delta E_{ex}(L_0,\beta) = E(L_0+1/2,\beta) - E(L_0-1/2,\beta) - E_{bulk}(\beta) \tag{20}$$

for L_0=8.5 and L_0=12.5. Going to high or low temperatures $\Delta E_{ex}(L_0,\beta)$ vanishes within error bars. Starting at high temperatures $\Delta E_{ex}(L_0,\beta)$ is decreasing with decreasing x until a minimum is reached at $x\approx 2.7$. Then at $x\approx 0$ a local maximum is assumed. The value of $\Delta E_{ex}(L_0,\beta)$ at this maximum is still negative. At a slightly smaller value of x there is a local minimum. Then at $x\approx -2.2$ the global maximum is reached.

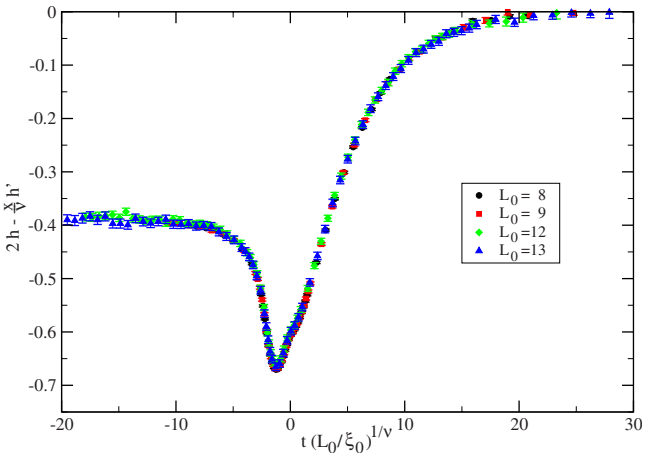

FIG. 2. (Color online) We plot $2h(x)-\frac{x}{\nu}h'(x)$, where $h'(x)$ is approximated by $E_{ex}(L_0,\beta)L_0^2[L_0/\xi_0]^{-1/\nu}$, as a function of $t[L_0/\xi_0]^{1/\nu}$ for L_0=8, 9, 12, and 13 for periodic boundary conditions. For a discussion see the text.

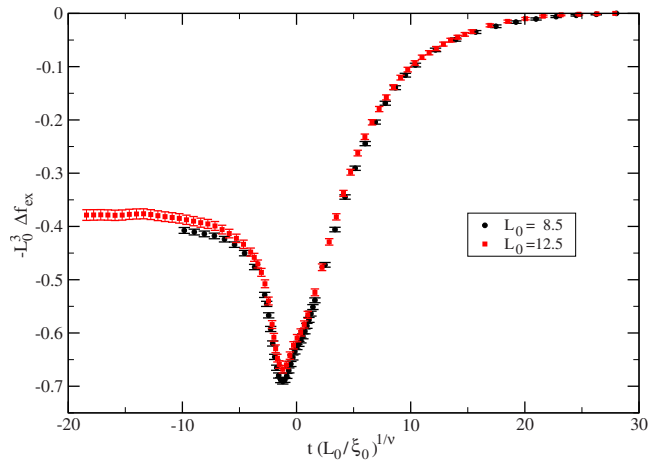

FIG. 3. (Color online) We plot $-L_0^3\Delta f_{ex}(L_0,\beta)$ as a function of $t[L_0/\xi_0]^{1/\nu}$ for L_0=8.5 and 12.5 for periodic boundary conditions. For a discussion see the text.

Using the trapezoidal rule we compute

$$-\Delta f_{ex}(L_0,\beta) = \int_{\beta_0}^{\beta} d\tilde{\beta}\Delta E_{ex}(L_0,\tilde{\beta}). \tag{21}$$

As initial values of the integration we have chosen $\Delta f_{ex}(8.5,0.35)=0$ and $\Delta f_{ex}(12.5,0.42)=0$. At these values of β, within error bars, $\Delta E_{ex}(L_0,\beta)$ is consistent with zero. Also here we have checked that systematical errors due to the finite step size of the numerical integration are negligible. Our results are plotted in Fig. 3. Here we see a small discrepancy between the results obtained from L_0=8.5 and L_0=12.5. Finally, in Fig. 4 we compare the results obtained from the two different approaches. In both cases we have plotted only the result obtained from the largest thickness, i.e., L_0=13 and L_0=12.5, respectively. These two results are consistent within error bars. Since corrections to scaling should be different in the two approaches, this gives us further confirmation that corrections to scaling are at most of similar size as our statistical errors.

Now let us discuss some characteristic features of $\theta(x)$: throughout $\theta(x)$ assumes negative values. In the high-temperature phase our results are consistent with the theoretical expectation that the thermodynamic Casimir force vanishes at sufficiently large x. In contrast, in the low-temperature phase $\theta(x)$ approaches a constant nonvanishing value. Averaging our results for L_0=12 and 13 and L_0=12.5 we arrive at $\theta_{low}=-0.384(10)$. The authors of Ref. 14 obtain from their simulations of the standard XY model $\theta_{low}=-0.383(3)$. These results are fully consistent with the exact result of the spin-wave approximation $\theta_{low}=-\zeta(3)/\pi=-0.3826\ldots$.[14]

The function $\theta(x)$ assumes a single minimum. The position of this minimum is given by the zero of $\Delta E_{ex}(L_0,\beta)$. We find $x_{min}=-1.206(18)$ and $x_{min}=-1.20(3)$ for L_0=8.5 and

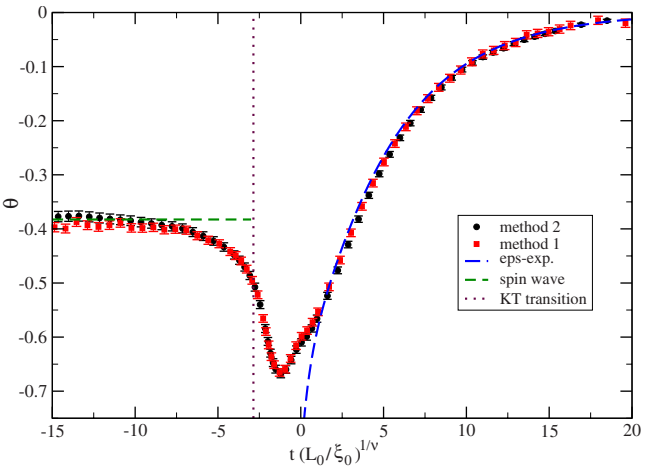

FIG. 4. (Color online) We plot $\theta(x)=2h(x)-\frac{x}{\nu}h'(x)$, where $h'(x)$ is approximated by $E_{ex}(L_0,\beta)L_0^2[L_0/\xi_0]^{-1/\nu}$ as a function of $t[L_0/\xi_0]^{1/\nu}$ for $L_0=13$ (method 1, red squares). For comparison we give $\theta(x)\simeq -L_0^3\Delta f_{ex}(L_0,\beta)$ for $L_0=12.5$ (method 2, black circles). In addition we give the result of the ε expansion (Ref. 16) (blue dashed line on the right side of the figure) and the spin-wave result (horizontal green dashed line on the left side of the figure). The vertical dotted line indicates the Kosterlitz-Thouless transition. Periodic boundary conditions are considered. For a discussion see the text.

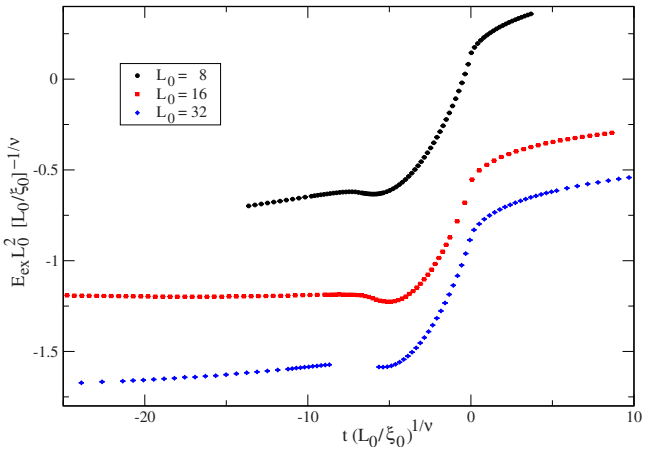

FIG. 5. (Color online) We plot $E_{ex}L_0^2[L_0/\xi_0]^{-1/\nu}$ as a function of $t[L_0/\xi_0]^{1/\nu}$ for thin films, where we have used $\xi_0=0.26362$ and $\nu=0.6717$. Free boundary conditions are considered. For a discussion see the text.

$L_0=12.5$, respectively. For the scaling limit we quote $x_{min}=-1.20(5)$, where the error also should include systematical errors due to corrections to scaling. The value of the scaling function at its minimum is given by $\theta_{min}=-0.66(2)$.

At the critical point of the bulk system we get $2h(0)=-0.607(2)$, $-0.606(3)$, $-0.599(6)$, and $-0.601(7)$ for $L_0=8$, 9, 12, and 13, respectively. The other method provides us with $-L_0^3\Delta f_{ex}(L_0,\beta_c)=-0.628(5)$ and $-0.612(7)$ for $L_0=8.5$ and 12.5, respectively. We conclude $\theta(0)=-0.60(2)$ for the scaling limit.

C. Previous simulations and field theoretic results

Dantchev and Krech[13] have simulated the standard XY model. The thicknesses of the films were $L_0=16$, 20, 24, and 32. They computed $\theta(x)$, up to an overall normalization, by using the stress tensor. They have fixed the missing normalization by imposing $\theta(0)=-0.56$, which they have obtained from theoretical considerations. Qualitatively, their result, which is presented in Fig. 5 of Ref. 13 is in agreement with ours. They do not quote results for x_{min} and $\theta(x_{min})$.

Also the authors of Ref. 14 have simulated the standard XY model. They have computed the free energy of thin films per area. They have studied films of a thickness up to $L_0=20$. Their results for $\theta(x)$ are plotted in Fig. 6 of Ref. 14. Qualitatively, their result agrees with ours. At the critical point they get $\theta(0)=-0.5986(14)$ and for the minimum of the scaling function they quote $x_{min}=-0.73(1)$ and $\theta(x_{min})=-0.633(1)$, where, in particular, x_{min} is clearly different from our result.

Krech and Dietrich[15] have computed the scaling function $h(x)$ in the high-temperature phase using the ϵ expansion up to $O(\epsilon)$. Later Grüneberg and Diehl[16] have extended the calculation up to $O(\epsilon^{3/2})$. In Fig. 4 we have plotted $\theta(x)$ obtained from the $O(\epsilon^{3/2})$ result of Ref. 16. Note that, following,[16] we have evaluated the result for three dimensions by naively setting $\epsilon=1$. The $O(\epsilon^{3/2})$ is in quite good agreement with our numerical data for $x\gtrapprox 1$. For $x\lessapprox 1$ the deviation rapidly increases with decreasing x. One should note that the difference between the $O(\epsilon)$ result[15] and the $O(\epsilon^{3/2})$ result[16] is smaller than our error bars (≈ 0.01) for $x\gtrapprox 3$. The $O(\epsilon)$ approximation has a minimum at $x\approx 0.75$.

V. FILMS WITH FREE BOUNDARY CONDITIONS

Here we study thin films with free boundary conditions in the short direction. These boundary conditions are relevant for the comparison with experimental results obtained for thin films of ^{4}He. Most of the Monte Carlo data are taken from our previous work,[17,20] where we have simulated films of the thicknesses $L_0=8$, 16, and 32. Therefore we refrain from giving the details of the simulations and refer the reader to Refs. 17 and 20.

Analogous to the previous section we compute the scaling function $h'(x)$ of the excess energy per area and $h(x)$ of the excess free energy per area. Using these we obtain the scaling function $\theta(x)=2h(x)-\frac{x}{\nu}h'(x)$ of the thermodynamic Casimir force.

In Ref. 17 we have taken great care to get the deviations of the energy per area from its effectively two-dimensional thermodynamic limit under control. In order to achieve this, quite large ratios L/L_0 are needed in the neighborhood of the peak of the specific heat. In the case of $L_0=8$ we have simulated lattices of a size up to $L=2048$, and for $L_0=16$ up to $L=1800$. For $L_0=32$ we have skipped the interval $0.5136<\beta<0.516$ since we could not simulate sufficiently large values of L.

In Fig. 5, similar to the previous section, we have plotted $E_{ex}L_0^2[L_0/\xi_0]^{-1/\nu}$ versus $t[L_0/\xi_0]^{1/\nu}$. In contrast to the previous section we find that there is a huge discrepancy between

TABLE I. The energy density E/L_0 of thin films of the thickness L_0 at the inverse critical temperature $\beta_c=0.5091503(6)$ of the three-dimensional systems. In all cases $L=6L_0$.

L_0	E/L_0
8	0.799566(31)
12	0.832786(19)
16	0.850727(13)
24	0.8698028(85)
32	0.8798552(57)
48	0.8903321(37)
64	0.8957662(29)

the three curves. The dominant effect seems that the curves are shifted by a constant with respect to each other. Note that replacing L_0 by $L_{0,eff}=L_0+L_s$ with $L_s=1.02(7)$ (Ref. 19) does change this situation only little. In Sec. III we have argued that the analytic background of the energy density might suffer from a boundary correction that is not given by the effective thickness $L_{0,eff}=L_0+L_s$ that describes the leading boundary corrections of singular quantities. Below we shall study this question in detail at the critical point of the bulk system, where we have data for thicknesses up to $L_0=64$ available.

A. Finite-size scaling at the critical point of the bulk system

In order to get a better understanding of the corrections we have studied in detail the behavior at the critical point of the three-dimensional bulk system. In the context of Ref. 17 we have simulated lattices of the thickness $L_0=8$, 12, 16, 24, 32, 48, and 64 and $L=6L_0$. In Ref. 17 we have checked that this choice of L is sufficient to approximate well the effectively two-dimensional thermodynamic limit of the film at the critical point of the three-dimensional system. Our results for the energy per area are summarized in Table I.

In the case of periodic boundary conditions in all directions, the energy density at the critical point behaves as

$$E(L) = E_{\rm ns} + cL^{-d+1/\nu}, \tag{22}$$

where $d=3$ is the dimension of the system. Using lattices of the size $L_0=L_1=L_2$ with L_0 up to 128 we find[30]

$$E_{\rm ns} = 0.913213(5) + 20\times(\beta_c - 0.5091503) + 5\times 10^{-7} \times (1/\alpha + 1/0.0151). \tag{23}$$

In order to take into account corrections due to the free boundary conditions of the thin film we use the ansatz

$$E(L_0) = (L_0 + L_{\rm sns})E_{\rm ns} + c_f L_{0,eff}^{-d+1+1/\nu} \tag{24}$$

to fit the data given in Table I. As input we have used $\nu=0.6717(1)$,[3] $E_{\rm ns}$ given in Eq. (23) and $L_s=1.02(7)$.[19] The parameters of the fit are $L_{\rm sns}$ and c_f. Fitting all data with $L_0\geq 8$ we get an acceptable χ^2 per degree of freedom. We find $L_{\rm ns}=-1.3529(3)$ when fixing $L_s=1.02$ and $L_{\rm ns}=-1.3523(3)$ fixing $L_s=0.95$. Hence $L_{\rm sns}$ is clearly different from L_s and it shows little dependence on the value taken for L_s. We have checked that the error of $L_{\rm sns}$ due to the uncertainties of ν and $E_{\rm ns}$ can be ignored.

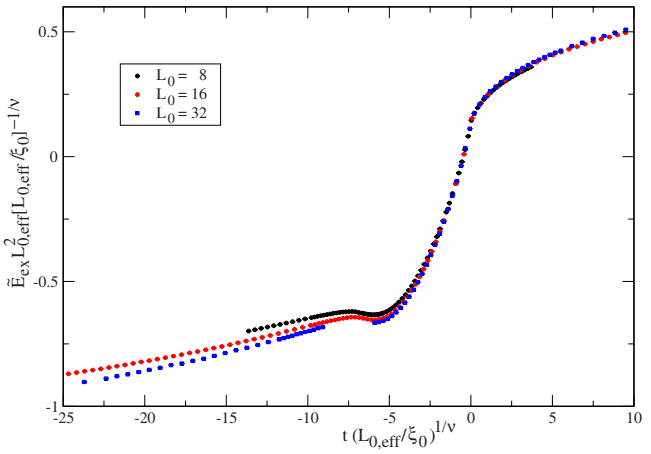

FIG. 6. (Color online) We plot $\tilde{E}_{ex}L_{0,eff}^2[L_{0,eff}/\xi_0]^{-1/\nu}$ as a function of $t[L_{0,eff}/\xi_0]^{1/\nu}$ for $L_0=8$, 16, and 32 for free boundary conditions. For a discussion see the text.

B. Taking into account boundary corrections

The boundary correction $L_{\rm ns}E_{\rm ns}$ should be an analytic function of the reduced temperature. In a first attempt we shall approximate it by its value at the critical point of the three-dimensional system found above. Hence in Fig. 6 we plot $\tilde{E}_{ex}L_{0,eff}^2[L_{0,eff}/\xi_0]^{-1/\nu}$, where

$$\tilde{E}_{ex} = E(L_0,t) - L_{0,eff}E_{bulk}(t) + (L_s - L_{\rm sns})E_{\rm ns} \tag{25}$$

as a function of $x=t[L_{0,eff}/\xi_0]^{1/\nu}$. Now we see a quite good matching of the three curves. Only for small x discrepancies are visible.

Next we have computed the finite-size scaling function θ of the Casimir force following Eq. (18). In the case of $L_0=8$ and $L_0=16$ we have used the function $h'(x)$ as given in Fig. 6. In the case of $L_0=32$ we have taken the missing part in the range $-5.9>x>-9.1$ from the results for $L_0=16$. To this end we have matched the values of the function at $x=-5.9$ and $x=-9.1$ resulting in $h'_{32}(x)=h'_{16}(x)+0.011-0.002(x+5.9)$ for $-5.9>x>-9.1$. We have computed the function $h(x)$ by numerically integrating $h'(x)$ using the trapezoidal rule. For sufficiently large x the Casimir force vanishes and therefore $h(x)=\frac{x}{2\nu}h'(x)$. Hence for large x,

$$h'(x) = cx^{2\nu-1}. \tag{26}$$

In Ref. 20 we found that the thermodynamic Casimir force is of similar size or smaller than the numerical errors that we achieve for $x\gtrapprox 4$. We have checked that in this range the scaling function $h'(x)$ of the excess energy indeed follows Eq. (26).

Hence we have started the numerical integration in the high-temperature phase at $x_0\approx 4$ with the starting value $h(x_0)=\frac{x_0}{2\nu}h'(x_0)$. In order to check the reliability of our result, we have redone the integration using a set of data points, where we have skipped every second value of β. We found

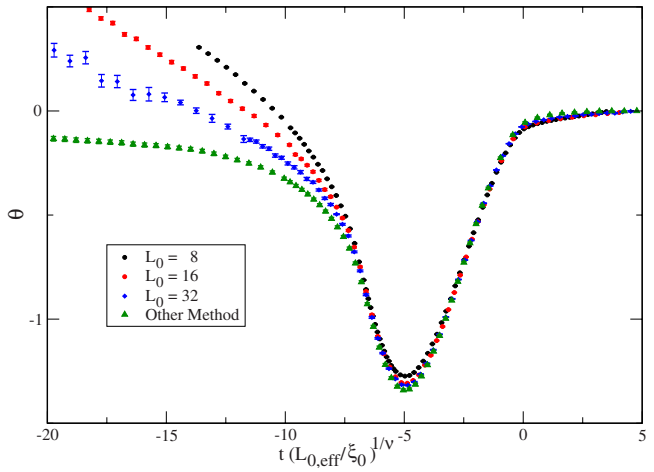

FIG. 7. (Color online) We plot finite-size scaling function θ of the thermodynamic Casimir force for free boundary conditions. We have computed θ from the finite-size scaling function h' of the excess energy per area of the film. For comparison we give the result of our previous work (Ref. 20) where we have computed θ directly from the thermodynamic Casimir force. For a discussion see the text.

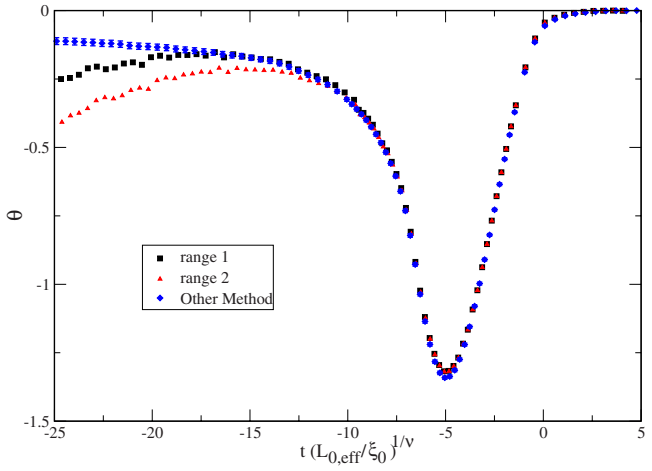

FIG. 8. (Color online) Similar to the previous figure. Here we have taken into account the analytic correction computing the scaling function h'. For a discussion see the text.

an agreement within the statistical errors. Our results for θ are plotted in Fig. 7. In the range $-7<x<5$ the curves obtained from the different values of L_0 match quite well. There is also a good match with θ obtained in Ref. 20. In particular, the value and the position of the minimum of θ are completely consistent. However for $x<-7$ the difference between the curves becomes clearly visible and increases with decreasing x. For small x, even for $L_0=32$ there is a huge discrepancy with the result of Ref. 20.

Since these discrepancies appear for large values of $|x|$ it is likely that they are mainly caused by analytic corrections. To check this explicitly, we allowed for two different types of corrections,

$$x = t(1 - ct)[L_{0,eff}/\xi_0]^{1/\nu} \tag{27}$$

and for a temperature dependence of the boundary correction of the analytic part of the energy

$$\tilde{E}_{ex} = E(L_0,t) - L_{0,eff}E_{bulk}(t) + (L_s - L_{sns})E_{ns} - c_b t. \tag{28}$$

We find that the curves for $h'(x)$ obtained from $L_0=16$ and $L_0=32$ can be nicely matched by adjusting the two parameters c and c_b. Matching in the interval $-18<x<3$ we find $c\approx-1.1$ and $c_b\approx-3.03$ and for the interval $-25<x<5$ $c\approx-0.75$ and $c_b\approx-2.97$. Using the corresponding results for $h'(x)$ we have computed the finite-size scaling function $\theta(x)$ that is plotted in Fig. 8. Now we see that the range of the matching with our previous result[20] is extended to $-15\gtrapprox x\gtrapprox 4$ in the case of the matching range $-25<x<4$. For still smaller values of x discrepancies rapidly increase. Likely higher-order analytic corrections are the main reason for this behavior. However also other types of corrections such as $t^{\nu\omega'}$ with $\omega'\approx 1.8$ (Ref. 37) should be taken into account. Therefore we abstain from fitting with t^2 corrections.

VI. SPECIFIC HEAT OF THIN FILMS OF ^{4}HE AND THE THERMODYNAMIC CASIMIR FORCE

In a number of experiments the excess specific heat of thin films of ^{4}He and ^{3}He-^{4}He mixtures has been measured in the neighborhood of the λ transition.[11] In these works the scaling function f_2 which is defined by

$$C_{bulk}(t) - C(L_0,t) \simeq L_0^{\alpha/\nu} f_2(tL_0^{1/\nu}) \tag{29}$$

is extracted from experimental data for the specific heat of the three-dimensional bulk system $C_{bulk}(t)$ and of thin films $C(L_0,t)$, where L_0 is the thickness of the film. Since the specific heat is the derivative of the energy density with respect to the temperature, $f_2(x)$ is, up to a constant factor, equal to $h''(x)$.

To compute this factor let us start from the excess reduced free energy density,

$$f(t,L_0) - f_{bulk}(t) \simeq L_0^{-3} h(x), \tag{30}$$

where $t=T/T_\lambda-1$ and $x=t[L_0/\xi_0]^{1/\nu}$. Note that here, as long as the free energy density and L_0^{-3} are measured in the same units, $h(x)$ is uniquely defined; there is no ambiguous factor.

The excess energy density is given by the derivative with respect to $\beta=1/(k_BT)$. Hence

$$E(t,L_0)/L_0 - E_{bulk}(t) = -L_0^{-3}[L_0/\xi_0]^{1/\nu}\frac{1}{k_BT_\lambda}\beta^{-2} \simeq -L_0^3[L_0/\xi_0]^{1/\nu}k_BT_\lambda, \tag{31}$$

where we have approximated $\beta^{-2}\simeq k_B^2T_\lambda^2$ in the neighborhood of the λ transition. The specific heat as defined in the experiments is given by the derivative of the energy density with respect to the temperature. Hence

$$C_{bulk}(t) - C(t,L_0) \simeq k_B L_0^{-3}[L_0/\xi_0]^{2/\nu} h''(x). \tag{32}$$

The results for the specific heat of the experiment are given in J mol^{-1} K^{-1}. These we convert into k_B Å^{-3} to get the same units on both sides of Eq. (32). Note that the thickness of the films in Refs. 26 and 27 is quoted in Å^{-3}. To this end

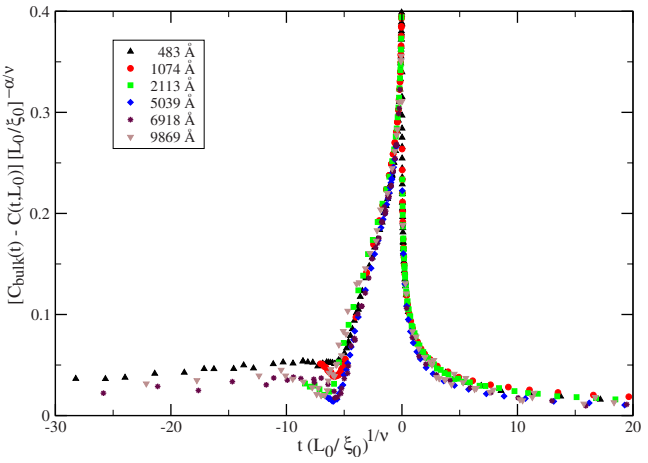

FIG. 9. (Color online) We plot $[C_{bulk}(t)-C(L_0,t)][L_0/\xi_0]^{-\alpha/\nu}$ as a function of $x=t[L_0/\xi_0]^{1/\nu}$. The data for thin films of ^{4}He of thicknesses 483, 1074, 2113, 5039, 6918, and 9869 Å obtained in Refs. 26 and 27 are taken from Ref. 39. Note that at the critical point $t=0$ the finite-size scaling function assumes the value ≈ 3.05. For a discussion see the text.

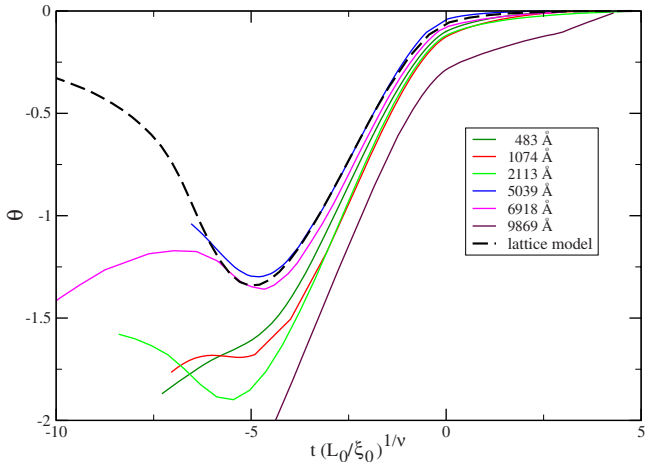

FIG. 10. (Color online) We plot results for the scaling function θ of the thermal Casimir force. These results were obtained by numerically integrating experimental data (Refs. 26, 27, and 39) for the excess specific heat of thin films of ^{4}He near the λ transition. For comparison we give the result obtained in Ref. 20. For a discussion see the text.

we need the density $\rho_\lambda=146.1087$ kg/m^3 (Ref. 38) of ^{4}He at the λ transition, the molar weight 4.0026… g mol^{-1} of ^{4}He and the Boltzmann constant $k_B=1.38065\ldots\times10^{-23}$ J K^{-1}. This amounts to the factor 0.00264… J^{-1} mol K k_B Å^{-3}. In Ref. 39 the data are given as a function of the reduced temperature $t=T/T_\lambda-1$, where $T_\lambda=2.17\ldots$ K. In order to plot them as a function of $x=t[L_0/\xi_0]^{1/\nu}$ we have used $\xi_0=1.422(5)$ Å which we[17] have computed from the amplitude of the bulk specific heat of ^{4}He at vapor pressure[40] and the universal amplitude ratio R_α.[31]

In Fig. 9 we have plotted

$$[C_{bulk}(t)-C(L_0,t)]k_B^{-1}L_0^3[L_0/\xi_0]^{-2/\nu} \tag{33}$$

as a function of $x=t[L_0/\xi_0]^{1/\nu}$. To this end we have used the data given in Ref. 39 for the thicknesses 483, 1074, 2113, 5039, 6918, and 9869 Å.[41]

Note that $h''(0)\approx 3.05$ as can be obtained from the results of Sec. 4.3 of Ref. 17. For $x\gtrapprox -5$ the curves obtained from different thicknesses of the film fall reasonably well on top of each other. It has been noticed[11] that for $x\lessapprox -5$, in particular, in the neighborhood of the minimum, the results obtained for different thicknesses differ by quite large factors. In Ref. 17 we have computed the specific heat and the scaling function f_2 starting from the data for the energy density discussed above. We find that for $x\lessapprox -5$ our final result is clearly smaller than the experimental ones.[26,27]

Starting from the results for the finite-size scaling function $h''(x)$ obtained from different thicknesses we have computed the scaling function $h'(x)$. To this end, we have applied the trapezoidal rule. Similar to the previous section, we have started the integration at $x_0\approx 4$ in the high-temperature phase. As starting value we have taken $h'(x_0)=\frac{x}{2\nu-1}h''(x_0)$. Again we have integrated $h'(x)$ using the trapezoidal rule to get $h(x)$. Here we have taken the same value for x_0 as above and $h(x_0)=\frac{x}{2\nu}h'(x_0)$. Using these results for $h'(x)$ and $h(x)$ we have computed $\theta(x)$ which we have plotted in Fig. 10.

In order to check the effect of errors due to the finite step size of the integration, we have repeated the integration, skipping every second value of x. In order to check the effect of the singularity of $h'(x)$ we have fitted the data for the specific heat in the neighborhood of the transition with the ansatz

$$h''(x)=3.05+c_\pm|x|^{-\alpha}. \tag{34}$$

Then we have integrated the ansatz in the neighborhood of the transition and compared it with the corresponding result from the trapezoidal rule. We find that the numerical results only change little and the conclusions drawn below are not effected.

Let us now discuss the results that we have obtained: for 483 Å the curve is monotonically decreasing with decreasing x; in particular, no minimum of the function can be observed. For 1074 Å a shallow minimum occurs at $x\approx -5.3$; for $x\lessapprox 6.1$ the function is decreasing again with decreasing x. For 2113 Å we see a clear minimum at $x\approx -5.5$; however the value of the minimum is clearly smaller than the one of Ref. 20. In the case of 5039 and 6918 Å we find a quite good match with our result[20] down to $x\approx -7$. For 6918 Å the minimum is located at $x\approx -4.8$ and the value of the minimum is $\theta\approx -1.3$. For 6918 Å the minimum occurs at $x\approx 4.65$ and the value of the minimum is $\theta\approx -1.36$. For 5039 Å no data for $x<-7$ are available. For 6918 Å the curve is decreasing again for $x\lessapprox -6.7$ with decreasing x. Up to here the expectation that with increasing thickness of the film the result converges toward the universal scaling function is fulfilled. However for the largest thicknesses studied, 9869 Å even the worst mismatch is found. The curve is monotonically decreasing with decreasing x and even for $x\gtrapprox 5$ there is quite large mismatch with our result for θ.[20] Playing around with the data, one finds that smaller values of $h''(x)$ for $x\lessapprox -5$ are needed to avoid that θ is decreasing with decreasing x for $x\lessapprox -5$. One should note that Eq. (8) only

holds for the scaling limit. Therefore the observations made here are not an indication that the experimental data are affected by an error. They can also be explained by corrections to the scaling behavior. This is at least true for the smaller thicknesses such as 483 Å. The result for 9869 Å is more puzzling. One should note that the analysis presented in this section does not depend on the type of boundary conditions that is realized in the experiment. But we think that the behavior of $\theta(x)$ for $x \lessapprox -5$ obtained here cannot be explained by different boundary conditions from those used in the study of the lattice model.[17,20]

VII. SUMMARY AND CONCLUSIONS

We have studied the relation of the excess specific heat and the excess energy with the thermodynamic Casimir force in thin films in the three-dimensional XY universality class. To this end we have exploited the relation (8),

$$\theta(x) = 2h(x) - \frac{x}{\nu} h'(x)$$

among the finite-size scaling functions $\theta(x)$ of the thermodynamic Casimir force, $h(x)$ of the excess free energy and $h'(x)$ of the excess energy. We have analyzed Monte Carlo data obtained for the energy per area of the improved two-component ϕ^4 model on the simple cubic lattice[17] and experimental results for the specific heat of thin films of ^{4}He near the λ transition.[26,27]

As a preparation we have simulated films with periodic boundary conditions. In contrast to Dirichlet boundary conditions periodic ones do not cause corrections to finite-size scaling. Indeed, we find a good collapse of the data for the excess energy per area already for the rather small thicknesses $L_0=8$, 9, 12, and 13 that we have simulated. Furthermore we find good agreement between $\theta(x)$ computed directly from the thermodynamic Casimir force, Eq. (6), and from the excess energy by using Eq. (8). We compare our result for $\theta(x)$ with previous ones[13,14] obtained from simulations of the standard XY model. We find a qualitative agreement between the results. However, for example, for the position of the minimum of $\theta(x)$ we find some discrepancy: While[14] quote $x_{min}=-0.73(1)$ we get $x_{min}=-1.20(5)$. Furthermore we find that the ϵ expansion[16] provides accurate results in the high-temperature phase down to $x \gtrapprox 1$.

Next we have analyzed the excess energy per area for films with free boundary conditions using the data obtained in Ref. 17. Here we find a huge mismatch between the thicknesses $L_0=8$, 16, and 32. Replacing L_0 by $L_{0,eff}=L_0+L_s$ with $L_s=1.02(7)$ (Ref. 19) does not remove this discrepancy. We argue that the nonsingular part of the energy per area suffers from boundary corrections that are not described by the same L_s which accounts for the corrections in singular quantities. Indeed, the analysis of the energy per area of films up to the thickness $L_0=64$ at the critical temperature of the three-dimensional system results in a L_{sns} for the analytic background of the energy per area that is clearly different from L_s. Taking into account this result we find a reasonable collapse of the finite-size scaling functions obtained from $L_0=8$, 16, and 32 in a large range of the scaling variable x.

Computing the Casimir force from this result for $h'(x)$ we find a good collapse for $-7 \lessapprox x < 4$. In this range of x we also find a good agreement with the result for θ that we have obtained in Ref. 20. Note that, in particular, the minimum of the scaling function θ is within this range. We confirm the position x_{min} and the value θ_{min} that we have obtained in Ref. 20. Next we took into account analytic corrections. The coefficients of these corrections were computed by matching the results obtained from $L_0=16$ and $L_0=32$. This way we could extend the range of agreement with our previous result[20] down to $x \approx -15$. This nice agreement gives us further confidence in the correctness of both θ computed in Ref. 20 as well as f_2 obtained in Ref. 17.

Finally we have computed the scaling function θ using experimental results for the excess specific heat.[26,27] Here we find a reasonable match with the theoretical results in the range $x \gtrapprox -5$. Only for four of the thicknesses a minimum is observed. These minima are located at $x_{min} \approx -5$ which is consistent with our prediction[20] but slightly larger than $x_{min}=-5.45(12)$ (Ref. 24) and $x_{min}=-5.7(5)$,[25] where the thermodynamic Casimir force has been determined for films of ^{4}He with thicknesses $\lessapprox 600$ Å. In the range $x \lessapprox -5$ the curves obtained from different thicknesses show quite different behavior. For the thicknesses 483 and 9869 Å the estimate of θ is monotonically decreasing with decreasing x. But also for the thicknesses 1074 and 6919 Å, eventually for smaller x the estimate of θ is decreasing with decreasing x. It is quite clear that this behavior is incorrect; it would mean that the thermodynamic Casimir force blows up with decreasing temperature. This is implausible and also ruled out by the experiments on the thermodynamic Casimir force.[24,25] One can figure out that this strange behavior of the estimate of θ corresponds to too large values of $h''(x)$ in the range $x \lessapprox -5$. Understanding this problem requires a detailed discussion of the experiments and is therefore beyond the scope of the present work.

ACKNOWLEDGMENT

This work was supported by the DFG under the Grant No. HA 3150/2-1.

*martin.hasenbusch@physik.hu-berlin.de

[1] M. E. Fisher and P.-G. de Gennes, C. R. Seances Acad. Sci., Ser. B **287**, 207 (1978).
[2] A. Gambassi, J. Phys.: Conf. Ser. **161**, 012037 (2009).
[3] M. Campostrini, M. Hasenbusch, A. Pelissetto, and E. Vicari, Phys. Rev. B **74**, 144506 (2006).
[4] K. G. Wilson and J. Kogut, Phys. Rep. **12**, 75 (1974).
[5] M. E. Fisher, Rev. Mod. Phys. **46**, 597 (1974).

[6] M. E. Fisher, Rev. Mod. Phys. **70**, 653 (1998).
[7] A. Pelissetto and E. Vicari, Phys. Rep. **368**, 549 (2002).
[8] M. N. Barber, in *Phase Transitions and Critical Phenomena*, edited by C. Domb and J. L. Lebowitz (Academic Press, New York, 1983), Vol. 8.
[9] *Finite Size Scaling and Numerical Simulation of Statistical Systems*, edited by V. Privman (World Scientific, Singapore, 1990).
[10] M. Barmatz, I. Hahn, J. A. Lipa, and R. V. Duncan, Rev. Mod. Phys. **79**, 1 (2007).
[11] F. M. Gasparini, M. O. Kimball, K. P. Mooney, and M. Diaz-Avila, Rev. Mod. Phys. **80**, 1009 (2008).
[12] M. Krech, *The Casimir Effect in Critical Systems* (World Scientific, Singapore, 1994).
[13] D. Dantchev and M. Krech, Phys. Rev. E **69**, 046119 (2004).
[14] O. Vasilyev, A. Gambassi, A. Maciolek, and S. Dietrich, Phys. Rev. E **79**, 041142 (2009).
[15] M. Krech and S. Dietrich, Phys. Rev. A **46**, 1886 (1992).
[16] D. Grüneberg and H. W. Diehl, Phys. Rev. B **77**, 115409 (2008).
[17] M. Hasenbusch, J. Stat. Mech.: Theory Exp. **2009**, P10006.
[18] H. W. Diehl, S. Dietrich, and E. Eisenriegler, Phys. Rev. B **27**, 2937 (1983).
[19] M. Hasenbusch, J. Stat. Mech.: Theory Exp. **2009**, P02005.
[20] M. Hasenbusch, J. Stat. Mech.: Theory Exp. **2009**, P07031.
[21] M. Hasenbusch, Phys. Rev. E **80**, 061120 (2009).
[22] A. Hucht, Phys. Rev. Lett. **99**, 185301 (2007).
[23] O. Vasilyev, A. Gambassi, A. Maciolek, and S. Dietrich, EPL **80**, 60009 (2007).
[24] R. Garcia and M. H. W. Chan, Phys. Rev. Lett. **83**, 1187 (1999).
[25] A. Ganshin, S. Scheidemantel, R. Garcia, and M. H. W. Chan, Phys. Rev. Lett. **97**, 075301 (2006).
[26] S. Mehta, M. O. Kimball, and F. M. Gasparini, J. Low Temp. Phys. **114**, 467 (1999).
[27] M. O. Kimball, S. Mehta, and F. M. Gasparini, J. Low Temp. Phys. **121**, 29 (2000).
[28] M. Campostrini, M. Hasenbusch, A. Pelissetto, P. Rossi, and E. Vicari, Phys. Rev. B **63**, 214503 (2001).
[29] M. Hasenbusch and T. Török, J. Phys. A **32**, 6361 (1999).
[30] M. Hasenbusch, J. Stat. Mech.: Theory Exp. **2006**, P08019.
[31] M. Hasenbusch, J. Stat. Mech.: Theory Exp. **2008**, P12006.
[32] J. M. Kosterlitz and D. J. Thouless, J. Phys. C **6**, 1181 (1973); J. M. Kosterlitz, *ibid.* **7**, 1046 (1974).
[33] M. Hasenbusch, J. Stat. Mech.: Theory Exp. **2008**, P08003.
[34] U. Wolff, Phys. Rev. Lett. **62**, 361 (1989).
[35] M. Saito and M. Matsumoto, in *Monte Carlo and Quasi-Monte Carlo Methods 2006*, edited by A. Keller, S. Heinrich, and H. Niederreiter (Springer, New York, 2008); M. Saito, M.S. thesis, Dept. of Math., Graduate School of Science, Hiroshima University, 2007. The source code of the program is provided at http://www.math.sci.hiroshima-u.ac.jp/~m-mat/MT/SFMT/index.html.
[36] N. Schultka and E. Manousakis, Phys. Rev. B **51**, 11712 (1995).
[37] K. E. Newman and E. K. Riedel, Phys. Rev. B **30**, 6615 (1984).
[38] R. C. Kerr and R. D. Taylor, Ann. Phys. **26**, 292 (1964).
[39] The data are linked at the bottom of the page, http://enthalpy.physics.buffalo.edu/Publications.html
[40] J. A. Lipa, J. A. Nissen, D. A. Stricker, D. R. Swanson, and T. C. P. Chui, Phys. Rev. B **68**, 174518 (2003).
[41] It would be interesting to repeat the analysis for other data sets as, e.g., those of Ref. 42.
[42] J. A. Lipa, D. R. Swanson, J. A. Nissen, Z. K. Geng, P. R. Williamson, D. A. Stricker, T. C. P. Chui, U. E. Israelsson, and M. Larson, Phys. Rev. Lett. **84**, 4894 (2000).